†Work supported in part by the U. S. Atomic Energy Commission.

[1]For example, A. E. Litherland, H. McManus, E. B. Paul, D. A. Bromley, and H. E. Gove, Can. J. Phys. 36, 378 (1958).
[2]A. Weidinger, R. H. Siemssen, G. C. Morrison, and B. Zeidman, Nucl. Phys. A108, 65 (1968).
[3]H. Fuchs, K. Grabisch, P. Kraaz, and G. Roschert, Nucl. Phys. A110, 65 (1968).
[4]G. A. Bissinger, P. A. Quin, and P. R. Chagnon, Nucl. Phys. A115, 33 (1968); A132, 529 (1969).
[5]J. F.Sharpey-Schafer, D. C. Bailey, P. E. Carr, A. N. James, P. J. Nolan, and D. A. Viggars, Phys. Rev. Letters 27, 1463 (1971).
[6]H. G. Price, A. N. James, P. J. Nolan, J. F. Sharpey-Shafer, P. J. Twin, and D. A. Viggars, Phys. Rev. C 6, 494 (1972).
[7]G. A. Bissinger and C. R. Gould, Particles Nuclei 3, 105 (1972).
[8]O. Hausser, T. K. Alexander, and C. Broude, Can. J. Phys. 46, 1035 (1968), O. Hausser and N. Anyas-Weiss, Can. J. Phys. 46, 2809 (1968).
[9]C. E. Moss, C. Detraz, and C. S. Zaidins, Nucl. Phys. A174, 708 (1971).
[10]J. W. Noe, D. P. Balamuth, R. R. Betts, H. T. Fortune, and R. W. Zurmuhle, Nucl. Phys. A186, 15 (1972).
[11]D. H. Youngblood, R. C. Bearse, N. Williams, A. E. Blaugrund, and R. E. Segel, Phys. Rev. 164, 1370 (1967).
[12]J. L. Durell, P. R. Alderson, D. C. Bailey, L. L. Green, M. W. Greene, A. N. James, and J. F. Sharpey-Schafer, J. Phys. A5, 302 (1972).
[13]G. A. P. Engelbertink and G. van Middlekoop, Nucl. Phys. A138, 588 (1969).
[14]C. E. Ragan, III, C. R. Gould, N. R. Roberson, G. E. Mitchell, and D. R. Tilley, Phys. Rev. C 3, 1152 (1971).
[15]A. E. Blaugrund, Nucl. Phys. 88, 501 (1966).
[16]J. Lindhard, M. Scharff, and H. E. Schiøtt. Kgl. Danske Videnskab. Selskab, Mat.-Fys. Medd. 33, No. 14 (1963).
[17]C. E. Ragan, III, Ph.D. dissertation, Duke University, 1970 (unpublished).
[18]C. Broude, P. Engelstein, M. Popp, and P. N. Tandon, Phys. Letters 39B, 185 (1972).
[19]R. A. I. Bell, J. L'Ecuyer, R. D. Gill, B. C. Robertson, I. S. Towner, and H. J. Rose, Nucl. Phys. A133, 337 (1969).
[20]S. J. Skorka, J. Hertel, and T. W. Retz-Schmidt, Nucl. Data A2, 347 (1966).
[21]E. K. Warburton and J. Weneser, in *Isospin in Nuclear Physics*, edited by D. H. Wilkinson (North-Holland, Amsterdam, 1969).
[22]P. M. Endt and C. van der Leun, private communication.

PHYSICAL REVIEW C VOLUME 7, NUMBER 3 MARCH 1973

Scattering of 9.8-MeV Neutrons from Silicon and Sulfur*

A. W. Obst†‡ and J. L. Weil
Department of Physics and Astronomy, University of Kentucky, Lexington, Kentucky 40506
(Received 20 September 1972)

Elastic and inelastic differential cross sections for neutron scattering from Si and S have been measured at an incident neutron energy of 9.8 MeV, using the high-energy neutron group from the ^{9}Be$(\alpha, n)^{12}$C source reaction. Due to the presence of the 4.439-MeV first-excited-state group from the ^{9}Be$(\alpha, n)^{12}$C* reaction only the scattering from the ground and first excited states in Si and S could be observed. Measurements were made on both elements by the time-of-flight technique in the angular region $20° \leq \theta_{lab} \leq 150°$ with an average neutron energy spread of 600 keV. The measured yields were corrected for flux attenuation, angular resolution, and multiple scattering. The cross sections were fitted by incoherently adding a compound-nuclear contribution to a direct-reaction contribution calculated by the optical-model-plus-distorted-wave–Born-approximation method and also by the coupled-channel method. Collective-model fits to S using oblate and prolate deformed rotational-model and vibrational-model form factors were all reasonably good. The fits to Si are not as good, possibly for reasons related to the large fluctuations in the neutron total and differential cross sections for Si in this energy region. The values of β obtained from these fits are, for the most part, consistent with those obtained from other measurements.

1. INTRODUCTION

There exists very little neutron scattering data in the energy range between 9 and 14 MeV, since most neutron scattering experiments done to date were performed using accelerators with less than 6-MeV energy, and the most prolific neutron source reactions, i.e., the T$(p, n)^3$He, D$(d, n)^3$He, and T$(d, n)^4$He reactions have Q values of −0.764, 3.266, and 17.586 MeV, respectively. In the range of energies from 9 to 14 MeV direct interactions are expected to begin to predominate over compound-nuclear processes for low-lying excited levels, and it is of interest to investigate the charac-

teristics of this transition region. Another feature of the scattering process worth studying is the model dependence of the direct contribution. The present work was undertaken as an extension of earlier measurements in this laboratory[1,2] in order to obtain information about neutron scattering in this unexplored energy region.

A secondary motivation was to try to extend the usefulness of a 6-MV Van de Graaff accelerator into this energy gap by investigating the feasibility of using the $^{9}Be(\alpha, n_0)^{12}C$ reaction ($Q = 5.704$ MeV), while performing the scattering experiments reported here. For the available bombarding energy, the $^{9}Be(\alpha, n)^{12}C$ reaction is the most prolific reaction producing neutrons in the energy range from 9 to 12 MeV.

The $^{9}Be(\alpha, n)^{12}C$ reaction has previously been used very little as a source of monoenergetic neutrons. Becker and Barschall[3] have used the n_0 neutron group for measuring total cross sections between 7.6 and 8.6 MeV. Several laboratories[4] have investigated the n_0 neutron group as a source of polarized neutrons. The cross sections for the $^{9}Be(\alpha, n)^{12}C$ reactions were measured in this laboratory and the results are presented by Obst, Grandy, and Weil[5] along with references to earlier work on this reaction. The 0° excitation function for the $^{9}Be(\alpha, n_0)^{12}C$ reaction has a large peak[5] at about 4.2-MeV bombarding energy. Therefore an α bombarding energy near this peak was used, giving a maximum yield with a mean neutron energy of 9.8 MeV.

The presence of neutron groups from excited states of ^{12}C beginning at 4.439-MeV excitation energy limits the investigation of levels in target nuclei to those with excitation energies below 4 MeV. Due to the relatively low neutron yield of the $^{9}Be(\alpha, n)^{12}C$ reaction it was necessary to use rather thick beryllium targets in order to obtain adequate statistics in a reasonable period of time. The over-all energy resolution resulting from the beryllium target thickness and the intrinsic time-of-flight spectrometer resolution was such that the scattering sample nuclei were limited to those having widely separated excited states. Silicon and sulfur were chosen, since the most abundant isotopes of these elements have isolated first excited states near 2 MeV.[6] Also previous investigations[7-13] have shown these excited states to be collective excitations, and it was thought worthwhile to observe the collective excitations in this new region of incident neutron energy. Natural samples of silicon (92.2% ^{28}Si, 4.7% ^{29}Si, 3.1% ^{30}Si) and sulfur (95.0% ^{32}S, 0.8% ^{33}S, 4.2% ^{34}S) were used as these are of relatively high isotopic purity and are also readily available. However, the high isotopic purity means that the present results are mainly representative of the most abundant components, ^{28}Si and ^{32}S.

2. EXPERIMENTAL METHOD

Solid beryllium targets were prepared by evaporating beryllium onto tantalum backings using resistive heating. The beryllium targets were weighed and mounted at the end of a wobbling target holder as shown in Fig. 1. The purpose of the wobbler was to distribute the beam over a larger portion of the target and thus to minimize target deterioration. A cold trap[5] was included in the target assembly in order to inhibit carbon deposition from cracked pump oil onto the beryllium target, which would have caused a decrease with time of the mean neutron energy. The detector shielding is also shown in Fig. 1. Standard time-of-flight techniques were used for the neutron detection and these have been described in Refs. 2 and 5. The flight path was 3.7 m from scatterer to detector.

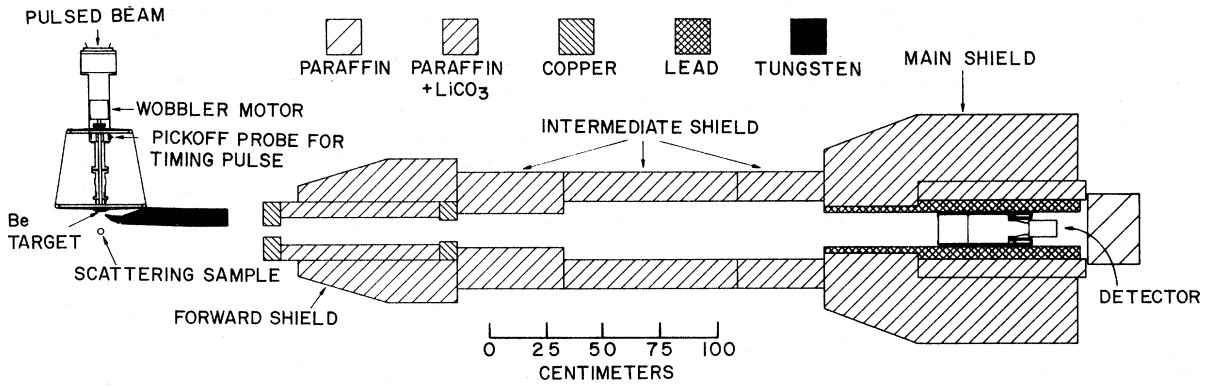

FIG. 1. Over-all view of neutron scattering apparatus showing detector shielding, neutron source, scatterer, and 12.5-cm×12.5-cm NE213 liquid scintillation detector mounted on a Phillips XP1040 photomultiplier.

The approximately right cylindrical scattering samples, whose dimensions are given in Table I, were positioned 9 cm from the beryllium target at 0° relative to the direction of the collimated α-particle beam. The samples were supported by a thin nylon monofilament fiber. The neutron flux was monitored by a small scintillation detector placed 1 m above the source in a polyethylene shield. Background runs at each angle were measured with the sample removed immediately before or after each sample-in run.

The variation of the detector efficiency with neutron energy was determined by measurements of the known 0° excitation functions and angular distributions of the $T(p,n)^3He$ and $D(d,n)^3He$ reactions.[14,15] The detector efficiency near 10-MeV neutron energy was obtained with the $D(d,n)^3He$ reaction by briefly raising the accelerator energy to 7 MeV. The detector bias was set on the full-energy peak of the 662-keV γ ray from ^{137}Cs, which corresponds to a neutron energy of about 2 MeV.

Measurements were made with a 770-keV-thick beryllium target and a 10-cm×5-cm NE 213 cylindrical liquid scintillation detector and also with a 530-keV-thick beryllium target and a 12.5-cm ×12.5-cm NE 213 cylindrical liquid scintillation detector. The thicker target produced neutrons with an energy spread of about 700 keV, while the thinner target produced neutrons with an energy spread of about 500 keV. The energy averages of the measured[16,17] neutron total cross sections at $E_n = 9.8$ MeV for Si and S differ by only 3 and 1%, respectively, when averaged over energy spreads of 700 keV and of 500 keV. For this reason, and since the present measurements of elastic scattering with the two different targets agreed within the experimental errors, the two sets of data on the elastic scattering cross sections were averaged together. However, the inelastic data taken with the 770-keV target were insufficiently reliable due to poor counting statistics and a relatively large neutron background from the source reaction. These data, taken with the smaller detector and shielding geometry described in Ref. 1, were therefore not averaged with the 530-keV-target inelastic data, which were taken with the improved shielding and detector arrangement shown in Fig. 1. The shielding geometry is not as critical for the elastic data, since at all angles where scattering was measured the elastically scattered neutrons have a higher energy than the source neutrons. The time-independent background was cut in half by the additional shielding used with the 530-keV target.

TABLE I. Neutron scattering sample sizes.

Material	Height (cm)	Diameter (cm)	Mass (g)
Sulfur	4.5	2.6	46.733
Silicon	3.7	2.6	49.374
Polyethylene	3.782	0.635 (o.d.) 0.079 (i.d.)	1.0893

3. DATA REDUCTION

A time-of-flight spectrum is shown in Fig. 2 for a scattering angle of 90°, as taken with the 530-keV target and the shielding geometry of Fig. 1. No isotopic corrections were made to any of the data, since neither the elastic yields nor the corresponding inelastic yields from the minor isotopes could be resolved from those of the major isotopes. Absolute data normalization was obtained by measuring n-p scattering from polyethylene at 35°, for which a time spectrum is shown in Fig. 3. In Fig. 3 can be seen the hydrogen and carbon peaks resulting from the scattering of both the ground- and first-excited-state neutron groups from the source reaction. The peak of interest here is the high-energy hydrogen peak in channel 327.

The differential elastic scattering cross sections were corrected for flux attenuation by the method of Cranberg and Levin,[18] for dead time in the counting electronics (never more than 1%) and for angular resolution and multiple scattering in the manner used by Reber and Brandenberger.[1,19] Flux-attenuation and dead-time corrections were also made to the inelastic scattering angular distributions, as well as a simplified multiple-scattering correction that accounted for the contribution (≈4%) to the inelastic cross section from those neutrons which had already been elastically scattered. The flux-attenuation corrections were 19 and 18% for the Si elastic and inelastic data, respectively, 16% for both the S elastic and inelastic data, and 7% for the polyethylene. The angular resolution correction was less than 10% at most angles except at the minima in Si at 50° where it was 31% and at the 50° minimum in S where it was 32%. The multiple-scattering correction was less than 5% at most angles except at the minima in Si at 50 and 105° where it was 20 and 7%, respectively, and at the minima in S at 50 and 105° where it was 8 and 7%, respectively. The uncertainty in the flux attenuation correction is about ±14% of the correction,[20] that in the angular resolution corrections is about ±10%, and that in the multiple-scattering correction is about ±20%.[19]

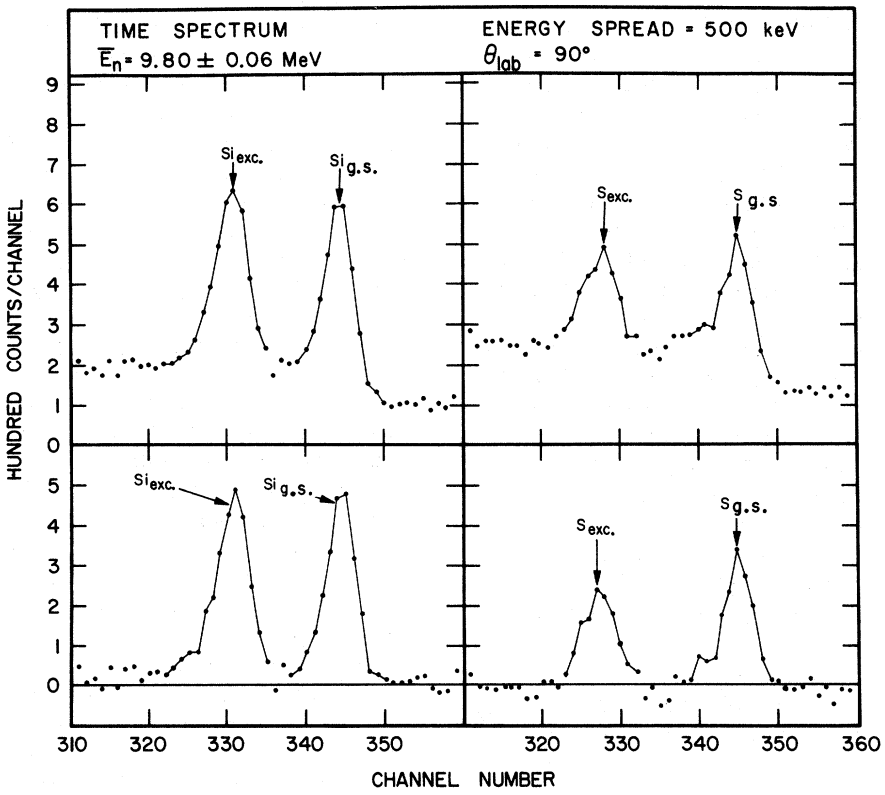

FIG. 2. Time-of-flight spectra for the high-energy neutron group from the $^{9}Be(\alpha,n)^{12}C$ reaction scattered from the ground and first excited states of Si and S at 90°. The top diagrams show the time spectra before background subtraction and the bottom diagrams show the time spectra after background subtraction.

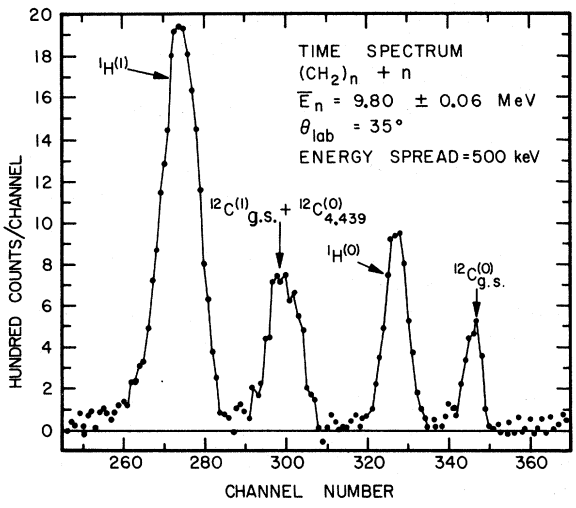

FIG. 3. Time-of-flight spectrum for the ground state and 4.439-MeV state neutron groups scattered from polyethylene $(CH_2)_n$. The low-energy carbon peak consists of ground-state neutrons from the $^{9}Be(\alpha,n)^{12}C$ reaction inelastically scattered from ^{12}C leaving $^{12}C^{*}_{4.439}$ plus the predominant first excited state neutron group from the $^{9}Be(\alpha,n)^{12}C^{*}_{4.439}$ reaction elastically scattered from ^{12}C.

The relative uncertainty in the elastic scattering differential cross sections varies with angle from ±3 to ±11% and in the inelastic scattering differential cross sections varies from ±4 to ±17%. The large relative uncertainties in the inelastic cross sections are due primarily to the large neutron background and to the uncertainty in this background. Other contributions to the relative errors are counting statistics (±1–11% in the elastic data taken with the 770-keV beryllium target, ±1–7% in the elastic data taken with the 530-keV beryllium target, and ±3–13% in the inelastic data) and the relative error in the cross sections due to uncertainty in the detector efficiency over the angular range of the distributions (≈±3%).

The uncertainty in the absolute normalization of the angular distributions is ±8% for the elastic data and ±6% for the inelastic data. The difference is due to the different energy spans covered on the efficiency curve between the energy of the neutrons scattered from hydrogen and the energy of the neutrons scattered elastically and inelastically from the scattering samples at 35° (angle of normalization). The contribution to the uncertainty in absolute normalization of the data from the er-

ror in the efficiency is ±7% for the elastic data and ±4% for the inelastic data. Other contributions to the absolute uncertainty are counting statistics in the n-p yield (±3%), error due to the uncertainty in the precise knowledge of the effective angle of neutrons scattered from polyethylene (±3%), and uncertainty in the n-p cross section[21] (±1%). The error in the effective angle of neutrons scattered from polyethylene was determined by the variation in the position of the hydrogen peak with respect to the adjacent carbon peaks in the time spectra taken at different times. The error in the scattering angle derived in this manner was estimated to be about ±2°, and is mostly due to uncertainty in the beam direction after passing through the buncher.

4. EXPERIMENTAL RESULTS

Angular distributions were measured for neutron elastic scattering from Si and S in the angular region $20° \leq \theta_{lab} \leq 150°$ and for neutron inelastic scattering to the first excited states in Si and S at about 2-MeV excitation energy, in the angular region $25° \leq \theta_{lab} \leq 150°$. The mean neutron bombarding energy was 9.80 ± 0.06 MeV. The average neutron energy spread for the elastic cross sections was about 600 keV (Sec. 2), while that for the inelastic cross sections was 500 keV. The elastic and inelastic scattering cross sections are shown in Figs. 4 and 5, respectively, with the same data shown throughout each column for comparison with various model calculations.

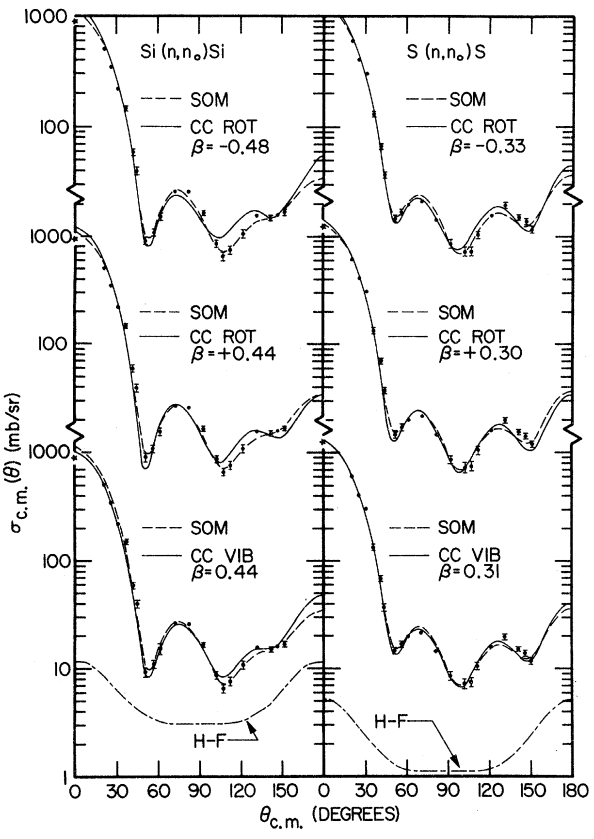

FIG. 4. Experimental neutron elastic scattering angular distributions for Si and S at 9.8 MeV. Relative errors are shown. The dashed and solid curves correspond to the optical model (SOM) and coupled-channel (CC) calculations, respectively, each plus a Hauser-Feshbach (HF) compound elastic contribution, which is also shown separately. All but the CC results are the same throughout each column. The optical-potential parameters are given in Table II. The asterisks at 0° indicate Wick's limit. The calculations in Figs. 4 and 5 are for ^{28}Si and ^{32}S.

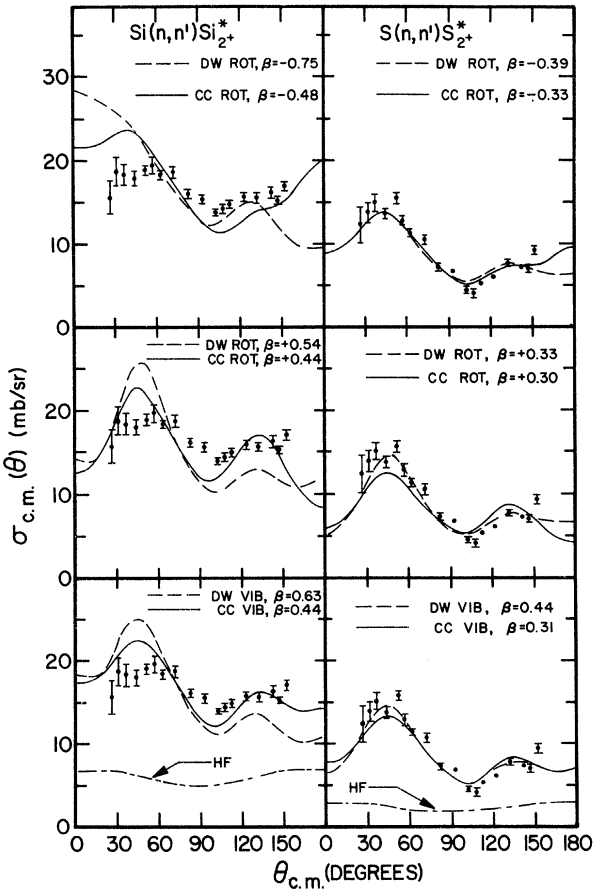

FIG. 5. Experimental neutron inelastic scattering angular distributions at 9.8 MeV to the first 2^+ states in Si and S. Relative errors are shown. The dashed and solid curves correspond to DWBA (DW) and coupled-channel (CC) calculations, respectively, each plus a Hauser-Feshbach contribution. The data and Hauser-Feshbach calculations (HF) are the same throughout each column. The optical potential parameters are given in Table II.

5. ANALYSIS AND DISCUSSION

A. Energy Dependence of the Cross Sections

The present experiment perforce gives scattering cross sections which are energy averaged over a large region of energy. Thus there is an opportunity to test the agreement between present theories of energy-averaged cross sections and this data. Energy averaging is important only insofar as it is necessary to account for the effect of that part of the cross section which varies rapidly with energy.

The standard theoretical formulation of energy-averaged compound-nuclear cross sections is Hauser-Feshbach[22] theory, and one of the main assumptions of this theory is that the random-phase approximation (RPA) is applicable. That is, it is assumed that the phases of the resonant scattering amplitudes are randomly distributed so that interference terms vanish upon energy-averaging.

Complementary to the Hauser-Feshbach theory of energy-averaged cross sections is the Ericson[23] theory of fluctuations which treats the effects of the interference of overlapping resonances when observed on a fine energy scale. The basic assumsumptions of the Ericson theory are that the level widths are randomly distributed and that the RPA is applicable.

The neutron total cross sections of both Si and S have been measured from 5 to 14 MeV with a 20-keV neutron energy spread by Carlson and Barschall.[16] Fluctuations are observed in the total cross sections of both nuclei, with the fluctuations being considerably larger for Si than for S. Their analysis shows that the cross-section fluctuations of both nuclei are consistent with the Ericson theory. More recently Grimes[17] has measured for neutron energies from 6.7 to 14 MeV the Si neutron total cross section, the 15 and 30° neutron elastic scattering differential cross sections, and the ^{28}Si(n, α) and ^{28}Si(n, p) angle-integrated excitation functions for the eight most energetic α and proton groups. The neutron energy spread of this work was 33 keV. Grimes[17] also concludes after considerable analysis that the fluctuation behavior of all the data is in agreement with Ericson theory. The correlation widths of the fluctuations in the energy range of the present experiment are 41 keV[16,17] for Si and 30 keV[16] for S.

Neutron elastic and inelastic scattering angular distributions for Si between 4- and 9-MeV bombarding energy[2,7,24,25] also exhibit fluctuations in shape and magnitude. These measurements were made with various energy spreads which were not much larger than the correlation widths observed by Carlson and Barschall[16] and Grimes.[17] The elastic and inelastic scattering angular distributions measured for S between 4 and 9 MeV[2,7,26] show smooth and progressive, rather than fluctuating, changes of shape as a function of neutron energy.

In order to separate the energy averaged and the fluctuating parts of the cross section, we follow the suggestion of Friedman and Weisskopf[27] and split the scattering amplitude into two parts:

$$S = \langle S \rangle + (S - \langle S \rangle) ,$$

where $\langle S \rangle$ is the smoothly varying shape elastic amplitude and $S - \langle S \rangle$ is the compound-nucleus amplitude which fluctuates with energy. If the RPA is valid, then as shown by John *et al.*,[28] the energy-averaged scattering cross section separates into an incoherent sum of two components:

$$\left\langle \frac{d\sigma}{d\Omega} \right\rangle = \frac{d\sigma_{se}}{d\Omega} + \frac{d\sigma_{ce}}{d\Omega} ,$$

where $d\sigma_{se}/d\Omega$ is the shape elastic cross section calculated either from the spherical optical-model or coupled-channel theory and $d\sigma_{ce}/d\Omega$ is the compound elastic cross section calculated from Hauser-Feshbach[22] theory. This incoherent sum for the average cross section has been fitted to the present data using a χ^2 criterion for best fit. Similar expressions apply to the nonelastic channels. Considering the experimentally determined validity of Ericson theory for Si and S at these energies and the fact that the RPA is assumed for both the Ericson and Hauser-Feshbach theories, this approximation of an incoherent sum of cross sections might be expected to be valid for the results of the present experiment, since the experimental energy averaging interval is 15–20 times the correlation width of the resonance levels.

B. Compound-Nuclear Contribution

The compound elastic and compound inelastic cross sections were calculated using the Hauser-Feshbach computer code ALTE.[29] The inelastic channels were not corrected for fluctuations in widths,[30] since at 9.8-MeV neutron energy the number of open channels is very large and therefore the width-fluctuation correction factor converges to 1. Since this energy region is also one of many strongly overlapping compound levels[17] the correlation enhancement factor in the compound elastic channels[30] converges to 2, and therefore the compound elastic cross sections were multiplied by 2. Of course, the nonelastic cross sections must suffer a corresponding reduction, but the reduction per channel is small because many channels are open.

The outgoing channels included in the compound-nuclear calculations were the (n, n_0), (n, n'), (n, p), and (n, α) channels. Known spins and parities of levels in the residual nuclei were taken from the compilation of Endt and van der Leun[6] and plausible values were assigned where not known. The random choice of unknown spins and parities, but maintaining the proper spin weighting, was found to have a negligible effect on the results of the Hauser-Feshbach calculations. The neutron potential parameters used in calculating the transmission coefficients were those used in the spherical optical-model fitting of the shape elastic data (see Sec. 5 C). The proton potential parameters were those proposed by Perey,[31] while the α potential parameters were taken from the work of Huizenga and Igo.[32] The Hauser-Feshbach contributions to the cross sections of interest were found to be relatively insensitive to reasonable variations of these potentials. This remark applies in particular to the neutron parameters, where no iteration between the compound elastic calculation and the shape elastic fits (see Sec. 5 C) was found necessary.

Hauser-Feshbach calculations were found by Grimes[17] to agree fairly well with 500-keV averages of the (n, p) and (n, α) cross sections for ^{28}Si for the four most energetic groups of each type of particle. This agreement implies that the (n, p) and (n, α) reactions are primarily compound-nuclear processes.

In the present work the sums over proton channels of the calculated (n, p) cross sections for both ^{28}Si and ^{32}S, corrected for the presence of a small direct-reaction contribution which is not differentiated against by the Hauser-Feshbach calculation (see following discussion and Sec. 5 E), were found to be in excellent agreement with the evaluated total (n, p) cross section.[33,34] The (n, α) cross section summed over α channels for ^{28}Si was found to be 25% lower than the evaluated total (n, α) cross section.[34] If the evaluated (n, α) cross section is correct, then the use of the Hauser-Feshbach value has resulted in an estimated 9% systematic error in the Si compound elastic and inelastic scattering cross sections. Since the (n, p) cross sections for both nuclei agreed well with the Hauser-Feshbach calculation and there were no (n, α) data available for ^{32}S in this energy range, the quality of the (n, α) prediction for ^{32}S was assumed to be the same as for ^{28}Si. If the true ^{32}S$(n, \alpha)^{29}$Al cross section is 25% higher than the Hauser-Feshbach calculated value, then the use of the calculated ^{32}S$(n, \alpha)^{29}$Al cross section has caused a 14% systematic error in the S compound elastic and inelastic scattering cross sections.

As noted above, following suggestions by Vogt[35] and Mittler[2] the compound-nuclear cross sections calculated from Hauser-Feshbach theory were corrected to remove the direct-reaction contribution to the total reaction cross section, since there is no discrimination between the two reaction mechanisms in the Hauser-Feshbach calculation. This was done by multiplying the uncorrected Hauser-Feshbach cross sections by

$$\frac{\sigma_a - \sigma_d}{\sigma_a},$$

where σ_a is the total absorption cross section and σ_d is the total direct reaction cross section. Using the evaluated[34] total inelastic scattering cross section, and assuming noninterference of the direct- and compound-nuclear contributions, the direct-reaction contribution for $\mathrm{Si}+n$ was calculated to be almost entirely due to inelastic scattering to the first 2^+ level (see also Sec. 5 E). This result was also used for S, since the information to make the analogous calculation was not available. The correction caused a 15% reduction in the Si compound cross sections and an 8% reduction in the S compound cross sections. The compound elastic and inelastic scattering cross sections are shown as the dash-dot curves in Figs. 4 and 5, respectively, and are the same throughout each column.

C. Elastic Scattering

The calculated compound elastic scattering cross section was subtracted from the elastic data and an optical-model fit, using the parameter search code JIB,[31] was made to the remaining measured shape elastic cross section. The form of the optical potential used was the Woods-Saxon for the real part and Woods-Saxon derivative for the imaginary part. A real spin-orbit potential of the Thomas form was also used. In searching for the best optical-potential parameters the starting values used were the global parameters used by Stelson *et al.*[8] and others. The three potential depths and the real diffuseness were varied simultaneously for various fixed values of the remaining parameters. The spin-orbit radius and diffuseness parameters were taken to be the same as for the real potential. The real radius parameter finally used was slightly smaller than the global value of 1.25 fm, while the imaginary radius and diffuseness parameters remained at their original values of 1.25 and 0.47 fm, respectively. The real diffuseness parameter was allowed to vary, since this might be expected to be larger than the standard value of 0.65 fm when a spherical-model potential is applied to a nonspherical nucleus.[9,36] The spherical-optical-model (SOM) parameters

finally arrived at are listed in Table II and the fits are shown in Fig. 4. Here the sums of the compound elastic and spherical-model shape elastic results are shown as dashed curves and are repeated in each graph for comparison with the other calculations.

The elastic scattering 0° differential cross section is related to the total cross section σ_T by Wick's limit,[37] σ_{WL}

$$\sigma_{c.m.}(0^\circ) \geq \sigma_{WL} = \left(\frac{k\sigma_T}{4\pi}\right)^2 ,$$

where k is the center-of-mass wave number. Wick's limit calculated from the measured total cross section[16,17] and averaged over 600 keV is plotted in Fig. 4, although it was not used as input in the fitting procedure. The fact that Wick's limit is always less than or equal to the calculated 0° cross section indicates that the present data and fits are consistent with the measured total cross sections and that there is no large systematic error[38] in the data.

The shape elastic scattering cross section has also been calculated using the coupled-channel formalism which has been reviewed in detail by Tamura.[39] The calculation was done with the ground-state scattering coupled to the scattering from the first excited 2^+ state using the computer code JUPITOR-1.[40] The solid curves in Fig. 4 correspond, from top to bottom, to the compound elastic plus the coupled-channel (CC) shape elastic calculations using oblate deformed, prolate deformed, and vibrational collective models, all with complex form factors. These form factors will be further discussed in Sec. 5 D.

The optical-model parameters used in the CC calculations were the same as in the uncoupled calculations except that the imaginary potential depth was reduced to better fit the elastic scattering distributions (see Table II). The imaginary well depth should be reduced,[39] since the first 2^+ state is now being explicitly taken into account, and need not be accounted for by W_D as in the uncoupled calculations. The uncoupled value of W_D for Si is somewhat larger than for S. The CC values of W_D, on the other hand, are similar for both nuclei. This difference in coupled and uncoupled values suggests that the 2^+ cross section for Si is larger than that for S, in qualitative agreement with the data (see Fig. 5).

D. Inelastic Scattering

Since ^{28}Si and ^{32}S are the dominant isotopes, the inelastic scattering will be discussed in terms of the 2^+ first excited states of these two nuclei, even though the data are for natural targets. The scattering from the first excited states of the minor isotopes is assumed to be enough similar that the results are not noticeably affected by the neglect of possible differences. The inelastic scattering data are shown in Fig. 5, with the same data repeated 3 times in each column. The cross section to the 2^+ level in ^{28}Si is measured to be about twice as large as the cross section to the 2^+ level in ^{32}S, consistent with the behavior of the absorptive potential in the elastic channel (see Sec. 5 C).

The inelastic scattering cross sections were analyzed by incoherently adding a Hauser-Feshbach contribution to a direct-reaction contribution calculated with either distorted-wave Born-approximation (DWBA) or coupled-channel formalisms. In the DWBA calculation the direct contribution was calculated using the computer code DWUCK.[41] Previous experiments[7-13] have shown the low-lying levels of ^{28}Si and ^{32}S to be collective excitations. Both rotational and vibrational models were tried in the fits to both nuclei, even though there is some evidence that the low-lying states in ^{28}Si form a rotational band with a negative ground-state deformation,[9,42] while the ^{32}S nucleus shows structure to be expected for a spherical vibrator nucleus.[9]

In the DWBA collective-model fitting procedure the deformed optical potential was expanded in a Taylor series about the mean radius. Generally

TABLE II. Optical-potential parameters. All depths in MeV, distances in fermis.

	V	r_R	a_R	W_D	r_I	a_I	V_{so}
Si	52.0	1.15	0.78 (SOM, DWBA)	12.1 (SOM, DWBA)	1.25	0.47	4.9
			0.78 (CC obl.)	7.5 (CC obl.)			
			0.78 (CC pro.)	8.0 (CC pro.)			
			0.76 (CC vib.)	7.0 (CC vib.)			
S	49.5	1.20	0.74 (SOM, DWBA)	10.3 (SOM, DWBA)	1.25	0.47	4.2
			0.74 (CC obl.)	8.0 (CC obl.)			
			0.74 (CC pro.)	8.5 (CC pro.)			
			0.74 (CC vib.)	8.0 (CC vib.)			

only the first-order term is retained to induce the excitation, but in the present work the second-order term[43] was also kept in the rotational model, since the deformation parameters β for ^{28}Si and ^{32}S are known[8] to be large ($\beta \geq 0.3$). In the vibrational model the second-order term is zero for a

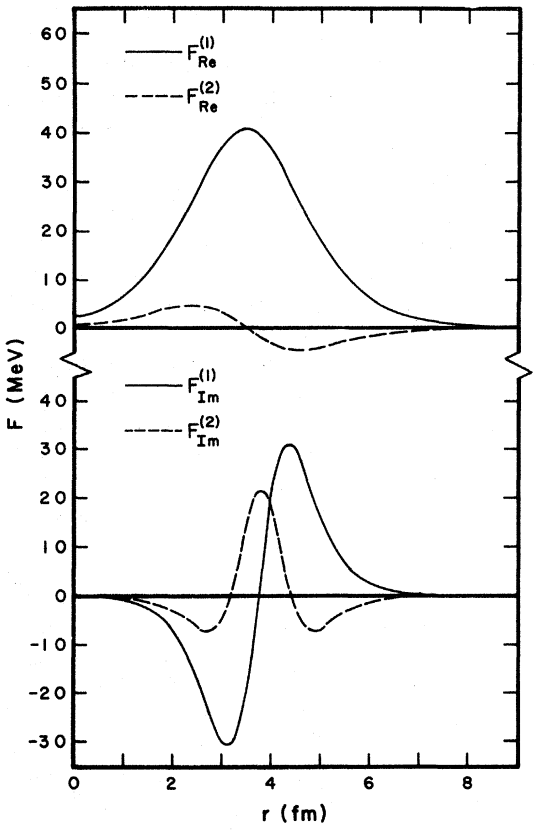

FIG. 6. Form factors used in the DWBA calculations for an oblate deformation ($\beta = -0.75$) in ^{28}Si. The equations and meanings of the curves are as follows: real first-order term,

$$F^{(1)}_{Re} = -\frac{\beta R_R V}{a_R}\frac{e^x}{(1+e^x)^2};$$

real second-order term,

$$F^{(2)}_{Re} = -\left(\frac{5}{196\pi}\right)^{1/2}\frac{\beta^2 R_R{}^2 V}{a_R{}^2}\frac{e^x(e^x-1)}{(1+e^x)^3};$$

imaginary first-order term,

$$F^{(1)}_{Im} = -\frac{\beta R_I W}{a_I}\frac{e^y(e^y-1)}{(1+e^y)^3},$$

imaginary second-order term,

$$F^{(2)}_{Im} = -\left(\frac{5}{196\pi}\right)^{1/2}\frac{\beta^2 R_I{}^2 W}{a_I{}^2}\frac{e^y(1-4e^y+e^{2y})}{(1+e^y)^4},$$

where

$$x = \frac{r-R_R}{a_R}, \qquad y = \frac{r-R_I}{a_I}.$$

one-phonon excitation, and it was found that mixing some two phonon contribution into the 2^+ excitation did not improve the fits to the data. The dashed curves shown in Fig. 5 correspond from top to bottom to the oblate deformed, prolate deformed, and vibrational models, each plus the same Hauser-Feshbach contribution. The optical-potential parameters used were the same as for the elastic scattering and only the deformation parameter β was adjusted to fit the data.

The first- and second-order form factors for the largest value of β encountered, -0.75 in the oblate deformation for ^{28}Si, are shown in Fig. 6, to illustrate that second-order terms are too large to be neglected. The second-order real form factor (top dashed curve) is small owing to the large real diffuseness (0.78 fm), while the second-order imaginary form factor (bottom dashed curve) is relatively large owing to the smaller imaginary diffuseness (0.47 fm). The second-order terms cause the differences between the oblate, prolate, and vibrational-model DWBA curves.

In the CC calculations shown by the solid curves in Figs. 4 and 5 the deformed optical potential in the oblate and prolate rotational models was expanded in a series of Legendre polynomials, rather than in the Taylor series as was done in the DWBA calculations. The Legendre expansion was restricted to a P_0 and a P_2 term. Also, the series expansion of the radius was truncated at the Y_2 term, since a Y_4 deformation in the shape did not improve the inelastic fits to the data. A need for a Y_4 deformation was found in some previous analyses[10] of 17.5- and 20.3-MeV proton scattering from ^{28}Si and ^{32}S.

The inelastic scattering fits to ^{28}Si and ^{32}S, determined by adjusting the deformation (or rms vibration) parameter β using a least-squares criterion, are of about the same quality for all three models. However, the fits to ^{28}Si are noticeably worse than for ^{32}S. It is possible that this difference is related to the fact that for bombarding energies from 5 to 8.5 MeV the shape of the Si(n, n_1)Si* angular distributions change rapidly[24] with energy, while those for S(n, n_1)S* do not.[26] Since the correlation width for Si is only 40 keV, it might be expected that the energy averaging which results from an incident neutron energy spread of 500 keV would remove the effects of such energy dependence. However, this does not appear to be the case in this instance.

The inclusion of coupling to higher excited states would probably have little effect on the 2^+ angular distributions, since the dominant direct contribution can be shown (see Sec. 5 E) to come from the first 2^+ excitation. Neither is it possible to explain the poor fit to ^{28}Si$(n, n_1)^{28}$Si* data on the basis

that the RPA is not valid here or that the energy dependence of the Si+n cross sections is due in part to the presence of intermediate structure, since both of these hypotheses have already been shown to be inapplicable in the work of Grimes[17] and Carlson and Barschall.[16]

In spite of the poor quality of the ^{28}Si inelastic fits, the coupled-channel fits to ^{28}Si (Fig. 5) are somewhat better than the DWBA fits, and the CC values of β (Fig. 5) are closer to the electromagnetic measurement[13,44] of 0.40 than are the DWBA β values. The CC and DWBA fits are comparable for ^{32}S and the β's are in reasonable agreement with the electromagnetic measurement[13] of 0.37. If one assumes that the models used are valid and neglects the poor quality of the ^{28}Si fit, the estimated uncertainty in the values of β determined here is ±10%. This error depends mainly on the uncertainty in the absolute cross sections, but includes a ±3% uncertainty in β due to the uncertainty in $\sigma^{HF}(n, \alpha)$ for both ^{28}Si and ^{32}S. The value of β from various other scattering experiments[7-12] for ^{28}Si ranges from 0.33 to 0.57 and for ^{32}S ranges from 0.20 to 0.40.

E. Neutron Cross Sections Integrated Over Angle

The angle-integrated elastic and inelastic scattering cross sections are presented in Figs. 7 and 8, respectively, along with data at neighboring neutron energies. The horizontal bars correspond to the energy spread in the data, where larger than the points. The vertical error bars, when not available, were taken to be ±10% for graphic illustration. The solid curve given by Drake[34] for Si in Fig. 7 corresponds to a 50-keV average of the measured neutron total cross section minus an evaluated nonelastic cross section. As discussed in Sec. 5A the fluctuations in the Si+n elastic channel are seen to be large up to 14-MeV bombarding energy. The inelastic curve for Si (Fig. 8) is a smooth line drawn[34] through the data available up to 1968. No such evaluation was available for S.

The angle-integrated elastic scattering data for Si generally fall close to the Drake curve. The inelastic data for Si taken since 1968 on the other hand fall well below the Drake curve. It can also

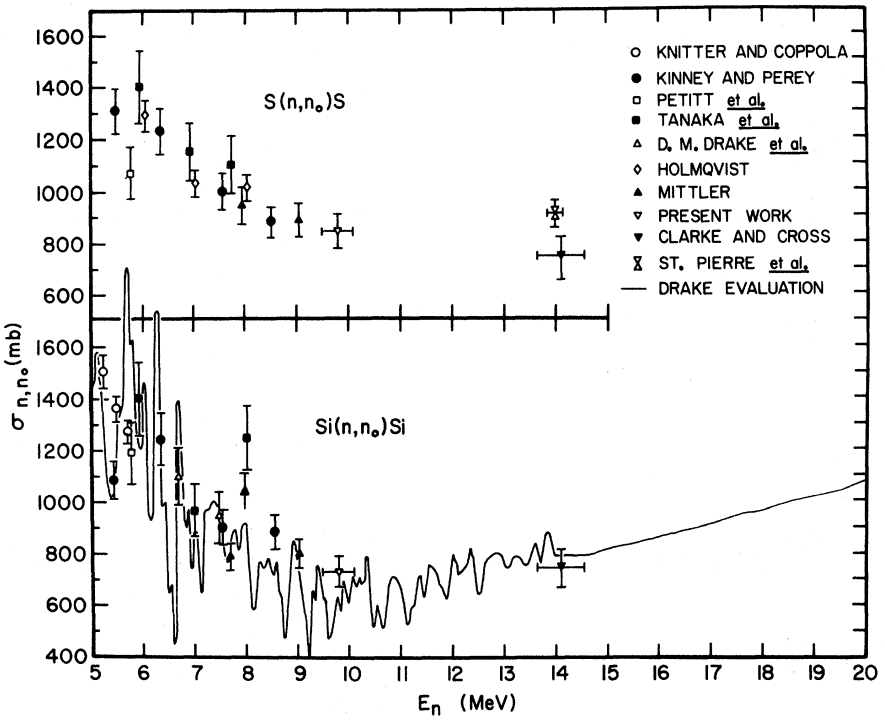

FIG. 7. Angle-integrated neutron elastic scattering cross sections for Si and S as a function of energy. The present results (▽) are shown along with the data of Knitter and Coppola (Ref. 25), Kinney and Perey (Refs. 24 and 26), Petitt *et al.* [Nucl. Phys. 79, 231 (1966)], Tanaka *et al.* (see Refs. 24 and 26), Drake *et al.* [Nucl. Phys. A128, 209 (1969)], Holmqvist [Arkiv Fysik 38, 403 (1969)], Mittler (Ref. 2), Clarke and Cross (Ref. 12), and St. Pierre *et al.* [Phys. Rev. 115, 999 (1959)]. The solid curve is the Drake evaluation (Ref. 34) averaged over 50-keV intervals.

be shown that the Drake evaluation of $^{28}Si(n, n')$-$^{28}Si^*_{1.78}$ is inconsistent with his evaluation[34] of the total (n, n') cross section by estimating the total direct interaction contribution at the energy of the present experiment. As discussed in Sec. 5B, the (n, α) and (n, p) channels are believed to proceed through the compound nucleus. In that case the direct contribution will be confined to the inelastic scattering channels. If we assume the incoherent addition of the compound and direct inelastic cross sections and correct the compound-nucleus contribution as was done before, then we have

$$\left(\frac{\sigma_a - \sigma^D_{nn'}}{\sigma_a}\right)\sigma^{HF}_{nn'} + \sigma^D_{nn'} = \sigma^T_{nn'} ,$$

where σ_a is the total absorption cross section, $\sigma^D_{nn'}$ is the direct interaction contribution to the total absorption cross section, $\sigma^{HF}_{nn'}$ is the summed inelastic scattering Hauser-Feshbach cross section taking into account only the compound elastic, compound inelastic, (n, p) and (n, α) channels, and $\sigma^T_{nn'}$ is the total inelastic scattering cross section. Using the values of $\sigma_a = 1200$ mb calculated from the optical model and of $\sigma^T_{nn'} = 625$ mb from Drake's evaluation[34] gives $\sigma^D_{nn'} = 127$ mb. Applying a similar expression to the inelastic scattering from the 1.78-MeV state alone gives $\sigma^D_{1.78} = 133$ mb, which is not inconsistent with the value calculated for $\sigma^D_{nn'}$. Here the angle-integrated inelastic cross section for $^{28}Si^*_{1.78}$ measured in the present experiment to be 207 mb was used for $\sigma^T_{1.78}$. If one uses Drake's estimate of $\sigma^T_{1.78} = 250$ mb, then one obtains $\sigma^D_{1.78} = 179$ mb which is inconsistent with the fact that $\sigma^D_{1.78} \leq \sigma^D_{nn'}$.

6. CONCLUSIONS

Neutrons with a mean energy of 9.8 MeV and a mean energy spread of 600 keV have been scattered from Si and S, using as a source the high-energy neutron group from the $^9Be(\alpha, n)^{12}C$ reaction. As can be seen in Figs. 7 and 8 these are the only data to the present time in the energy range between 9 and 14 MeV. The elastic scattering cross sections for Si and S have been fitted by incoherently adding to the shape elastic cross section, determined with reasonable optical-potential

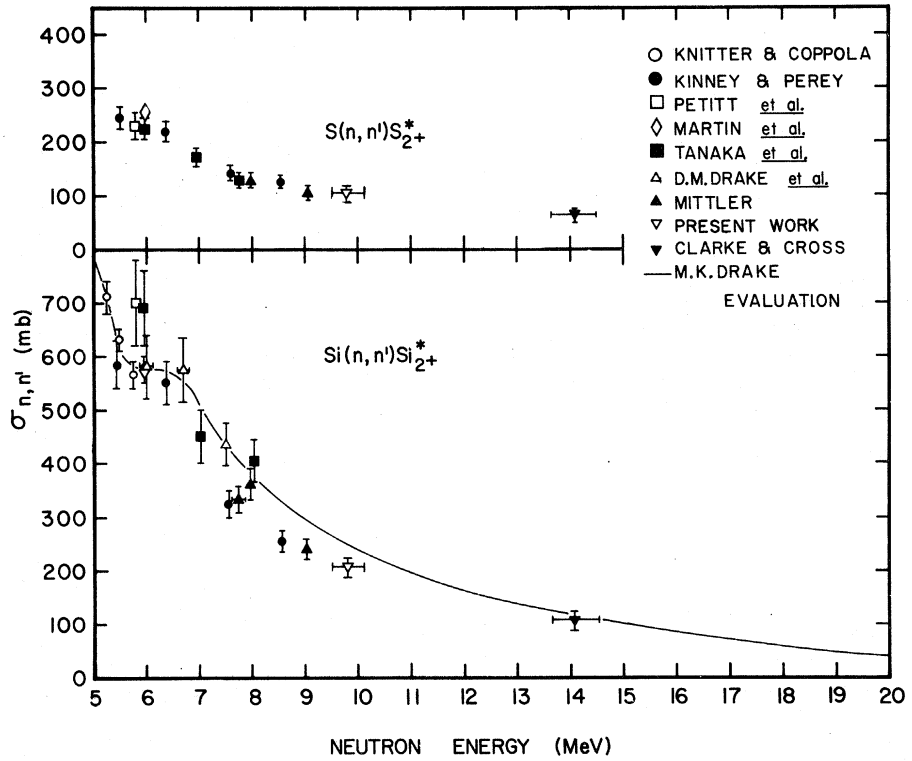

FIG. 8. Angle-integrated neutron inelastic scattering cross sections to the first 2^+ states in Si and S as a function of energy. The present results (▽) are shown along with the data of Knitter and Coppola (Ref. 25), Kinney and Perey (Refs. 24 and 26), Petitt *et al.* [Nucl. Phys. 79, 231 (1966)], Martin *et al.* (Ref. 7), Tanaka *et al.* (see Refs. 24 and 26), Drake *et al.* [Nucl. Phys. A128, 209 (1969)], Mittler (Ref. 2), and Clarke and Cross (Ref. 12). The solid curve of Drake (Ref. 34) is a smooth line drawn through data available up to 1968.

parameters, a compound-nuclear contribution determined from Hauser-Feshbach theory. The inelastic scattering angular distribution from the first 2^+ state in Si does not agree very well with an incoherent addition of a Hauser-Feshbach compound contribution to a direct contribution as determined from either a DWBA or CC calculation using collective-model form factors, although the latter does give a slightly better description of the data. This inability to fit the Si inelastic scattering data may be related to the large fluctuations present in the neutron total and differential cross sections for Si up to a neutron bombarding energy of 12 MeV. The S inelastic scattering angular distribution to the first 2^+ state, on the other hand, is fitted reasonably well with either the DWBA or CC theory added incoherently to a Hauser-Feshbach compound inelastic scattering contribution. In spite of the difficulties with the ^{28}Si fits, the values of β obtained for the first excited states of ^{28}Si and ^{32}S are for the most part consistent with the values obtained in other types of measurement.

It is also concluded that using the ^{9}Be$(\alpha, n)^{12}$C reaction as a source of high-energy neutrons is difficult, but feasible. The lower-energy groups limit the range of inelastic scattering that can be observed and the use of a thick target to reduce running time limits the energy resolution. It is not clear that using a large neutron energy spread is effective in removing the effects of fluctuations in the cross section as a function of energy.

ACKNOWLEDGMENTS

The authors wish to thank Professor M. T. McEllistrem, Professor J. D. Brandenberger, and Professor W. J. McDonald for many helpful discussions during the course of this work. The assistance of K. Sinram, Dr. T. B. Grandy, and the technical staff is greatly appreciated. We also wish to acknowledge the University of Kentucky Computing Center for their cooperation and for providing computing time for data reduction and analysis.

---

*Work supported in part by a grant from the National Science Foundation.

†Present address: Department of Physics, Florida State University, Tallahassee, Florida 32306.

‡Work performed in partial fulfillment of the requirements for the Ph.D.

[1]J. D. Reber and J. D. Brandenberger, Phys. Rev. 163, 1077 (1967).

[2]A. Mittler, Ph.D. dissertation, University of Kentucky, 1970 (unpublished); J. D. Brandenberger, A. Mittler, and M. T. McEllistrem, Nucl. Phys. A196, 65 (1972).

[3]R. L. Becker and H. H. Barschall, Phys. Rev. 102, 1384 (1956).

[4]B. P. Lietz, S. F. Trevino, A. F. Behof, and S. E. Darden, Nucl. Phys. 67, 1288 (1957); Th. Stammbach, G. Spalek, J. Taylor, and R. L. Walter, Nucl. Instr. Methods 80, 304 (1970); T. R. Donoghue, private communication.

[5]A. W. Obst, T. B. Grandy, and J. L. Weil, Phys. Rev. C 5, 738 (1972).

[6]P. M. Endt and C. van der Leun, Nucl. Phys. A105, 1 (1967).

[7]J. Martin, D. T. Stewart, and W. M. Currie, Nucl. Phys. A113, 564 (1968).

[8]P. H. Stelson, R. L. Robinson, H. J. Kim, J. Rapaport, and G. R. Satchler, Nucl. Phys. 68, 97 (1965).

[9]M. C. Mermaz, C. A. Whitten, Jr., and D. A. Bromley, Phys. Rev. 187, 1466 (1969).

[10]R. de Swiniarski, C. Glashauser, D. L. Hendrie, J. Sherman, A. D. Bacher, and E. A. McClatchie, Phys. Rev. Letters 23, 317 (1969); A. G. Blair, C. Glashauser, R. de Swiniarski, J. Goudergues, R. Lombard, B. Mayer, J. Thirion, and P. Vaganov, Phys. Rev. C 1, 444 (1970).

[11]F. Hintenberger, B. Mairle, U. Schmidt-Rohr, G. J. Wagner, and P. Turek, Nucl. Phys. A115, 570 (1968).

[12]R. L. Clarke and W. G. Cross, Nucl. Phys. 53, 177 (1964).

[13]P. H. Stelson and L. Grodzins, Nucl. Data A1, 21 (1965).

[14]J. E. Brolley, Jr., and J. L. Fowler, in *Fast Neutron Physics*, edited by J. B. Marion and J. L. Fowler (Interscience, New York, 1960), Pt. I, p. 73.

[15]M. D. Goldberg, private communication.

[16]A. D. Carlson and H. H. Barschall, Phys. Rev. 158, 1142 (1967).

[17]S. M. Grimes, Nucl. Phys. A124, 369 (1969).

[18]L. Cranberg and J. S. Levin, Los Alamos Scientific Laboratory Report No. LA-2177, 1959 (unpublished).

[19]J. D. Reber, Ph.D. dissertation, University of Kentucky, 1967 (unpublished).

[20]W. Galati, Ph.D. dissertation, University of Kentucky, 1969 (unpublished).

[21]J. D. Hopkins, Los Alamos Scientific Laboratory Report No. LA-DC-11039, 1969 (unpublished).

[22]W. Hauser and H. Feshbach, Phys. Rev. 87, 366 (1952).

[23]T. Ericson, Phys. Rev. Letters 5, 430 (1960); Ann. Phys. (N.Y.) 23, 390 (1963).

[24]W. E. Kinney and F. G. Perey, Oak Ridge National Laboratory Report No. ORNL-4517, 1970 (unpublished).

[25]H. H. Knitter and M. Coppola, Z. Physik 207, 56 (1967).

[26]W. E. Kinney and F. G. Perey, Oak Ridge National Laboratory Report No. ORNL-4539, 1970 (unpublished).

[27]F. L. Friedman and V. F. Weisskopf, in *Niels Bohr and the Development of Physics*, edited by W. Pauli (Pergamon, London, 1955), p. 134.

[28]J. John, C. P. Robinson, J. P. Aldridge, and R. H. Davis, Phys. Rev. 177, 1755 (1969).

[29]W. R. Smith, Comput. Phys. Commun. 1, 181 (1970);

Oak Ridge National Laboratory Report No. ORNL-TM-1117, 1965 (unpublished); Oak Ridge National Laboratory Report No. ORNL-TM-1234, 1965 (unpublished).

[30]P. A. Moldauer, Rev. Mod. Phys. 36, 1079 (1964); Massachusetts Institute of Technology Report No. MIT-2098-149, 1965 (unpublished).

[31]F. G. Perey, Phys. Rev. 131, 745 (1963).

[32]J. R. Huizenga and G. I. Igo, Argonne National Laboratory Report No. ANL-6373, 1961 (unpublished).

[33]*Neutron Cross Sections,* compiled by J. R. Stehn, M. D. Goldberg, B. A. Magurno, and R. Wiener-Chasman, Brookhaven National Laboratory Report No. BNL-325 (U. S. GPO, Washington, D. C., 1964), Suppl. 2.

[34]M. K. Drake, Gulf General Atomic Report No. GA-8628, 1969 (unpublished); See also J. K. Dickens, Phys. Rev. C 2, 990 (1970).

[35]E. Vogt, Advan. Nucl. Phys. 1, 261 (1968).

[36]T. Tamura, J. Phys. Soc. Japan, Suppl. 24, 288 (1968).

[37]G. C. Wick, Atti reale acad. Italia, Mem. Classe Sci. Fis., Mat. Nat. 13, 1203 (1943); Phys. Rev. 75, 1459 (1949).

[38]R. W. Bauer, J. D. Anderson, and L. J. Christensen, Nucl. Phys. 48, 152 (1963).

[39]T. Tamura, Rev. Mod. Phys. 37, 679 (1965).

[40]T. Tamura, Oak Ridge National Laboratory Report No. ORNL-4152, 1967 (unpublished).

[41]P. D. Kunz, University of Colorado (unpublished).

[42]F. C. P. Huang and D. K. McDaniels, Phys. Rev. C 2, 1342 (1970).

[43]R. H. Bassel, R. M. Drisko, and G. R. Satchler, Oak Ridge National Laboratory Report No. ORNL-3240, 1962 (unpublished).

[44]T. K. Alexander, C. Broude, A. J. Ferguson, J. A. Kuehner, A. E. Litherland, R. W. Ollerhead, and P. J. M. Smulders, in *Proceedings of the International Conference on Nuclear Physics, Gatlinburg, Tennessee, 1966,* edited by R. L. Becker (Academic, New York, 1967), p. 367.